are nearly indistinguishable for the leafy trees (which of course is the normal state of foliage.) As with the scattering effects, we see not only that the difference between the two frequencies is negligible, but the losses in the millimeter wave band in general (including 28 GHz) are very large: over 30 dB for a single foliated tree. Therefore, propagation through foliage, as with propagation by scattering, must be avoided in either of the two bands.

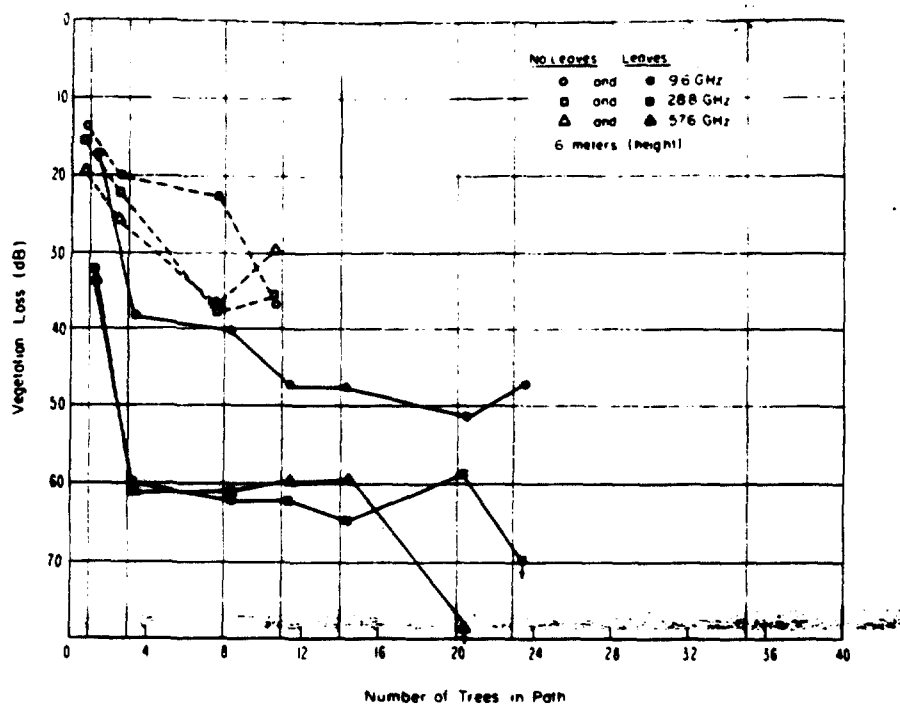

Exhibit 13. Foliage attenuation measurements

<u>Conclusion for 41.5 GHz Tree and Other Foliage Attenuation</u>

CellularVision assumed value:	Cell size reduction by factor of 2
Correct value:	No cell size reduction

Rain Backscatter [35]

CellularVision claims that rain backscatter increases with the frequency change from 28 to 42 GHz, resulting in increased interference in CellularVision receivers. Just the opposite trend is true, however. Exhibit 14[36] shows that the backscatter (equivalent to reflectivity) of rain falling at various rates *drops* in power level as frequency increases from 30 to 40 GHz. These results use the Mie scattering theory (which is the exact electromagnetic solution for drops of spherical shape) and realistic Laws-Parsons raindrop size distributions. These results do not include the attenuation introduced during propagation through the rain. The bulges at the higher altitudes in the 30 GHz curves represent the so-called "bright-band", where melting snow and ice particles produce especially strong backscatter. This analysis represents a realistic simulation of rain backscatter and conclusively refutes the allegation by CellularVision.

Conclusion for 41.5 GHz Rain Backscatter

CellularVision assumed value:	Cell size reduction
Correct value:	No cell size reduction

[35] See page 10 of LMDS is Not Viable

[36] See J. P. V. Poiares Baptista, General Editor, OPEX Second Workshop of the OLYMPUS Propagation Experimenters, Volume 4: Reference Book on Radar, ESA WPP-083, Nov 1994, Figures V.7,V.8

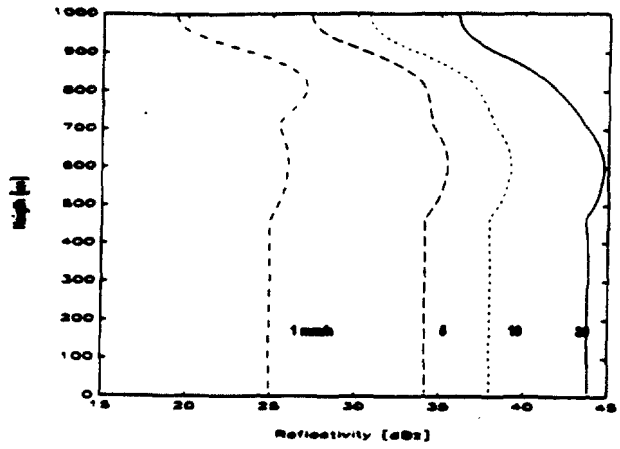

(a) Frequency = 30 GHz

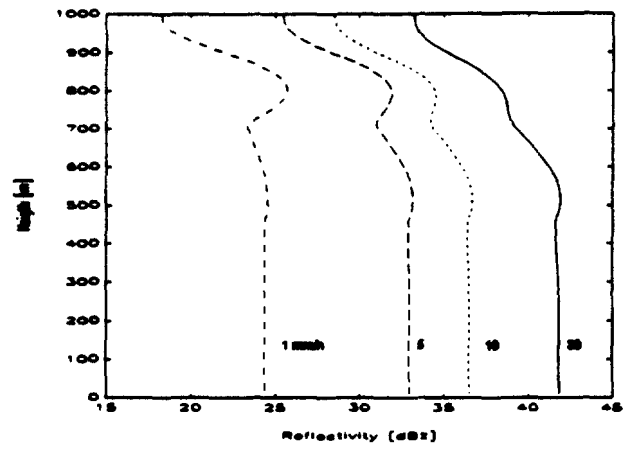

(b) Frequency = 40 GHz

Exhibit 14. Reflectivity (backscatter) of rain with altitude

Real Estate Considerations[37]

Since we have clearly shown that the number of hubs will not be increased due to increase in frequency, there are no additional costs related to real estate for placement of the hubs.

Conclusion for 41.5 GHz Real Estate Considerations

CellularVision assumed value:	Additional costs
Correct value:	No additional costs

[37] See page 10 of LMDS is Not Viable

6. FSS VS LMDS AT 41 GHZ

Key Differences between LMDS and Satellite on Point - Point Paths[38]

We have shown above that the scattering and foliage differences between the two bands are negligible, leaving rain loss as the only effect with an appreciable difference. CellularVision argues here on pg. 20 of Appendix 2, and again in Appendix 3, Item 13, that FSS links encounter a shorter rain path than LMDS links and therefore will experience less of an impact. A simple calculation disproves this assertion. In order to estimate the rain path on a satellite link, the vertical extent of the rain must be estimated. The Crane global model for rain attenuation[39] includes a statistical model for rain height; by this model at 40 degrees latitude and 99.9% availability, rain extends to a height of 3.2 km, or 2.0 miles. An FSS link with a 30 degree elevation angle will pass through 2.0/sin(30), or 4.0 miles of rain, while CellularVision specifies a 3 mile cell, so for this typical scenario the opposite of the CellularVision argument is true and FSS experiences a greater impact. The elevation angle at which the rain paths are equal in length is 41.8 degrees. Since FSS systems will use elevation angles both above and below this value (CONUS coverage from domestic GEO's require elevation angles of 30 to 50 degrees), neither LMDS nor FSS would consistently experience the greater impact due to rain attenuation at 42 GHz.

---

[38] See page 20 of LMDS is Not Viable, and Item 13 of Appendix 3 in same source

[39] See R. K. Crane, "Prediction of attenuation by rain," *IEEE Trans. Communications*, Vol. COM-28, No. 9, Sept 1980.

7. CONCLUSIONS

This report has demonstrated conclusively that the claims and arguments made by CellularVision that the 40.5 - 42.5 GHz frequency band is not suited for LMDS type service are completely unfounded and are not based on sound analytical, experimental and market evidence. The "7.3 factor" for the number of cells, and the "30 to 40 times" cost increase factor, are both fiction. CellularVision claims about non-line of sight operation, tree and foliage attenuation, rain backscatter, and FSS vs LMDS rain attenuation differences were all shown to be technically incorrect.

A reasoned and thorough evaluation of the elements of these claims has shown that LMDS service in the 40.5 - 42.5 GHz band is viable with the SAME cell sizes as proposed for 28 GHz operation, and at costs which initially may be 5 to 10% higher, but within a few years will be essentially identical. Therefore, in terms of both performance and system costs, the 40.5 -42.5 GHz band is a viable alternative to the 28 GHz band for LMDS service.

By: Louis J. Ippolito

Louis J. Ippolito
Thomas A. Russell
Julie H. Feil
Stanford Telecom
1761 Business Center Drive
Reston, VA 22090
(703) 438-8000

March 1, 1995

APPENDIX A

Electromagnetic Scattering about a Building Corner in an LMDS System

The Uniform Geometric Theory of Diffraction (UTD) has been implemented to determine the scattered electric field pattern due to a building in both a 28.5 GHz and a 41.5 GHz LMDS system. Classic geometric optics has been implemented to determine the incident and reflected electric field patterns.

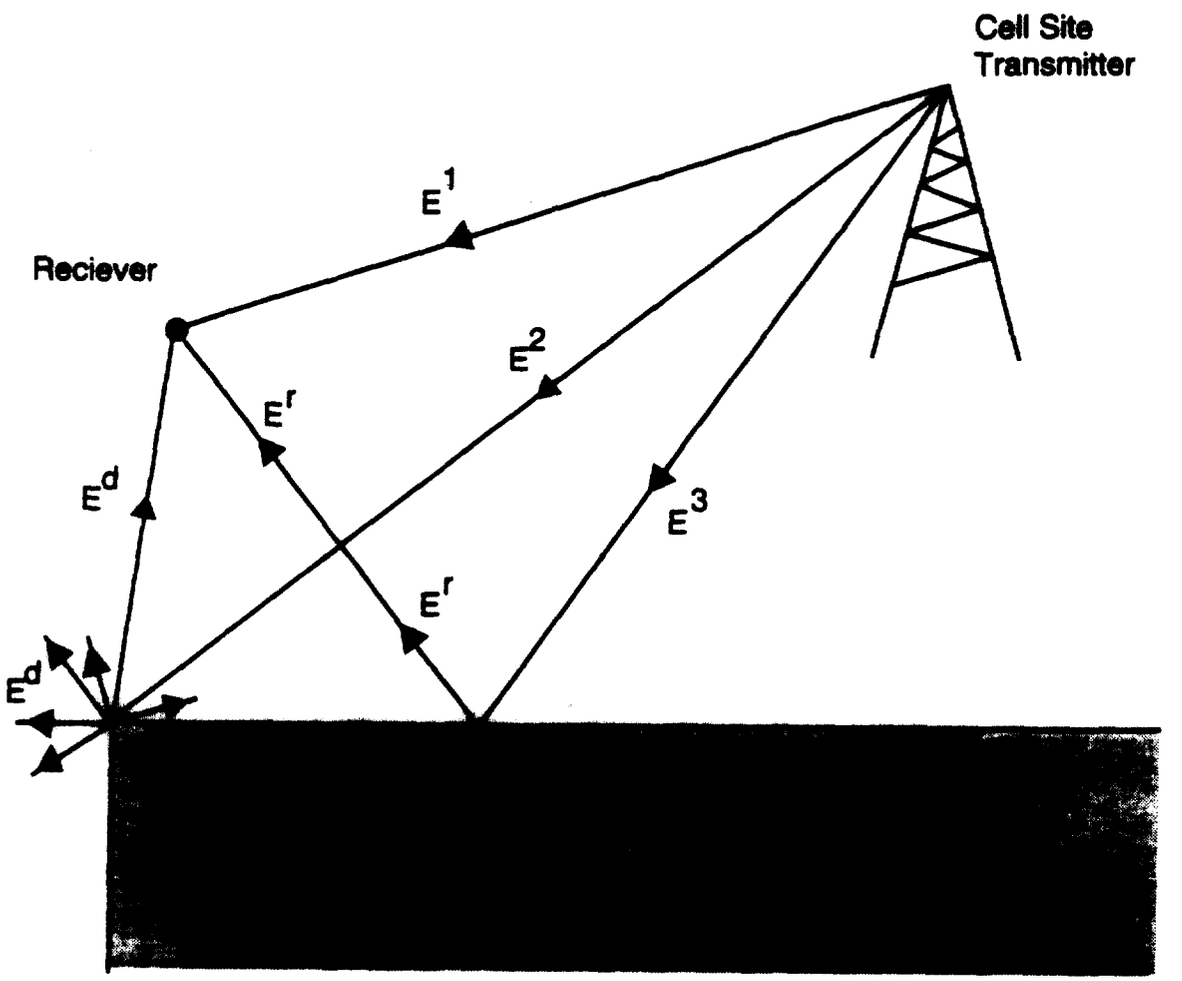

Exhibit A-1. Ray paths from cell site transmitter to receiver in presently of building.

Exhibit A-1 illustrates the LMDS broadcast cell site in the presents of a building which blocks part of the cell's coverage area. The incident electric field is assumed to radiate in an uniform omni-directional pattern from the cell site antenna. Exhibit A-1 illustrates the electric field ray paths from the cell site antenna to a possible receiver. The E^1 path simply propagates directly from the cell site antenna toward the receiver; this energy is the incident electric field, E^i. The E^2 path is more complicated since it bumps or reflects off the building; this reflected energy E^r then propagates toward the receiver. Since the building is not a pure conductor, some of the energy will be transmitted into the building; this transmitted energy is E^t. The E^3 path is the most complicated since it bumps into the building corner which causes the electric field to scatter or diffract; this diffracted energy E^d then propagates away from the building corner in all directions, including toward the receiver. Thus, the electric field at the receiver is the combination of the incident, reflected, and diffracted electric fields.

As previously stated, the incident, reflected, and transmitted electric fields can be calculated by classic geometric optics while the diffracted electric field is calculated by Uniform Geometric Theory of Diffraction (UTD). Since the wavelength at 28.5 GHz is .011 m and at 41.5 GHz is .0073 m, the building is considered electrically large; and a two dimensional approximation is reasonable. The source is assumed to be a line source; and the incident electric field radiates uniformly in an omni-directional pattern. The reflected and transmitted fields are calculated by Snell's Law. The reflection coefficient is determined from the test measurement previously referenced in Section 4 Non-Line of Sight Considerations.[A-1] Exhibit A-2 restates these reflection coefficients.

[A-1] E.J. Violette, R.H. Espeland, R.O. Debolt, F. Schwering, "Millimeter-wave propagation at street level in an urban environment," *IEEE Transactions Geoscience and Remote Sensing*, Vol. 26, No. 3, May 1989.

Frequency	Loss	Reflection Coefficient
GHz	dB	
28.5	11.2	0.274
41.5	13.0	0.244

Exhibit A-2. Reflection Coefficients from a typical building.

The diffracted field is the redirection of energy which scatters or diffracts from surface discontinuities such as a building corner. The diffracted field calculation is two dimensional UTD diffraction from a dielectric wedge.[A-2] The reflection coefficients in Exhibit A-2 were implemented in the diffraction coefficient.

Exhibit A-4 illustrates the key parameters for the diffracted field calculations. The building is modeled as a dielectric wedge in which the sides are considered infinitely long. This assumption is again due to the fact that the building is electrically large. The source location (cell site antenna) is defined in terms of s' and ϕ'. s' is the distance from the source to the diffraction corner, and ϕ' is the angle between the source incident ray and the edge of the building. The receiver or observation point location is defined in terms of s and ϕ. s is the distance from the building corner to the receiver, and ϕ is the angle between the building edge and the receiver. s' is assumed to be 1000m from the building, andϕ' is assumed to be 45 degrees. Since the problem is to determine the radiation pattern around a building corner, s remains constant at 30 m while ϕ varies from 0 to 270 degrees. The building or dielectric wedge is for ϕ equal to 270 to 360 degrees. Exhibit A-3 summarizes these values.

[A-2] V. Erceg, A.J. Rustako, R.S. Roman, "Diffraction Around Corners and Its Effects on Microcell Coverage in Urban Environments at 900 MHz, 2 GHz, and 6 GHz," *IEEE Transactions on Vehicular Technology*, Vol. 43, No. 3, August 1994. and W.D. Burnside, K.W. Burgener, "High Frequency Scattering by a Thin Lossless Dielectric Slab," *IEEE Transactions on Antennas and Propagation*, Vol. AP-31, No. 1, January 1983.

	Parameter	Value
Source	s'	1000 m
Source	ϕ'	45 degrees
Receiver	s	30 m
Receiver	ϕ	0 - 270 degrees
Building	ϕ	270 - 360 degrees

Exhibit A-3. Geometric parameters for diffraction from building in Exhibit A-4.

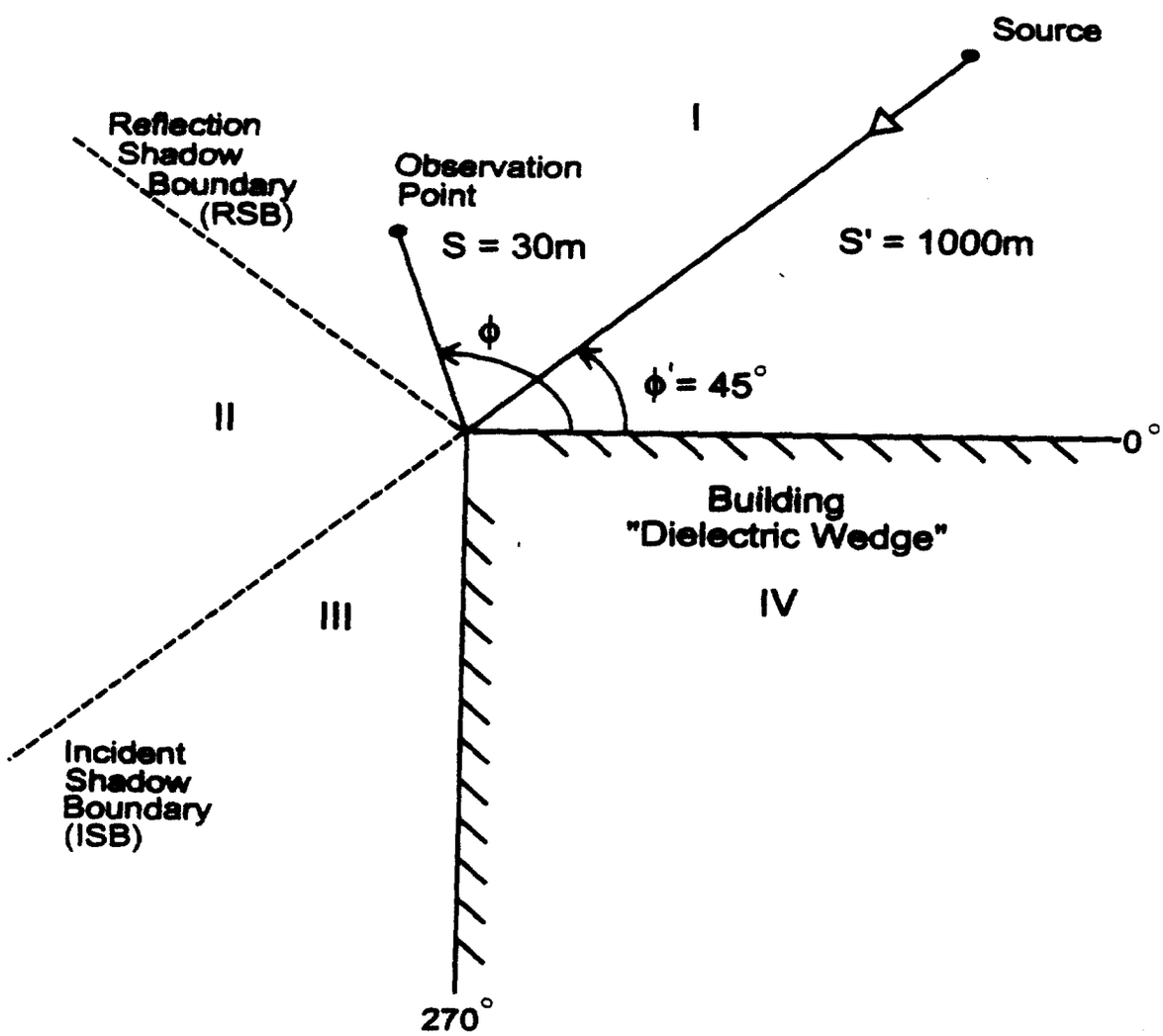

Exhibit A-4. Diffraction from a dielectric wedge.

As seen in Exhibit A-4, the Incident Shadow Boundary (ISB) is the boundary between where the incident electric field propagates and where it ceases to exist (the incident shadow region). Similarly, the Reflection Shadow Bound (RSB) is boundary between where the reflected electric field propagates and where it ceases to exist (the reflection shadow region); the RSB is determined by Snell's Law and the source location. For this case, ISB and RSB are defined in terms of ϕ. The ISB is located at 180 degrees plus ϕ' while the RSB is located at 180 degrees minus ϕ' as seen in Exhibit A-5.

Boundaries	**ϕ locations (degrees)**
ISB	180 + ϕ'
RSB	180 - ϕ'

Exhibit A-5. ISB and RSB locations.

The diffracted field radiates omni-directionally (but not uniformly) from the diffraction corner. Exhibit A-6 tabulates Exhibit A-4's four different regions (I, II, III, IV) in terms of their ϕ boundaries and their propagating electric fields.

Region	ϕ (degrees)	Electric fields
I	0 - RSB	$E^i + E^r + E^d$
II	RSB - ISB	$E^i + E^d$
III	ISB - 270	E^d
IV	270 - 360	$E^d + E^i$

Exhibit A-6. Electric field regions around the building corner.

Four different graphs are presented to analyze the electric fields' radiation pattern around the building corner. For each graph, the electric field value (in dB) is plotted against ϕ (in degrees), which represents the receiver location, since s remains constant. For these graphs, the parameters in Exhibit A-3 and

Exhibit A-4 are implemented. Each plot is labeled with respect to the regions illustrated in Exhibit A-4 and tabulated in Exhibit A-6. All electric field values are normalized with respect to the incident electric field.

Exhibit A-7 illustrates the 28 GHz incident, reflected, and diffracted electric field values for receiver locations about the building corner. Unless the receiver location is very close to the building, the reflected field is about 11 dB below the incident field. The diffracted field pattern shape requires an explanation of geometric optics and UTD. By geometric optics, the incident and reflected electric fields are discontinuous at their respected shadow boundaries; but experimentation and the Fresnel-Kirchhoff Diffraction Theory reveal that the field values are not discontinuous but rather have steep roll offs, and UTD is a numerical computation which corrects the geometric optics values for total electric field values. As discussed in Section 4, Fresnel-Kirchhoff Diffraction Theory describes this roll-off more accurately. The UTD diffracted field (neglecting the transition regions) peaks around ϕ equaling 180 degrees when the diffracted field is about 26 dB below the incident field. Exhibit A-8 illustrates the total 28.5 GHz electric field values about the building corner. By superposition, the total electric field value is the addition of the incident, reflected and diffracted field values in vector form. The oscillation of the Region 1 electric field is mainly due to the interaction between the incident and reflected electric fields. The diffracted field in Region I also contributes to the oscillation; but since the diffracted field is so far below the incident and reflected fields, the diffracted field is a minor contributor. The slight oscillation in Region II electric field values is due to the interaction between the incident and diffracted fields. Region III illustrates the steep roll off between the incident field and diffracted field as previously discussed. The diffracted field decreases about 1dB per degree in the incident shadow region. Region III also illustrates that the diffracted field is significantly lower than the incident field; therefore, subscribers in Region III would require very sensitive receivers.

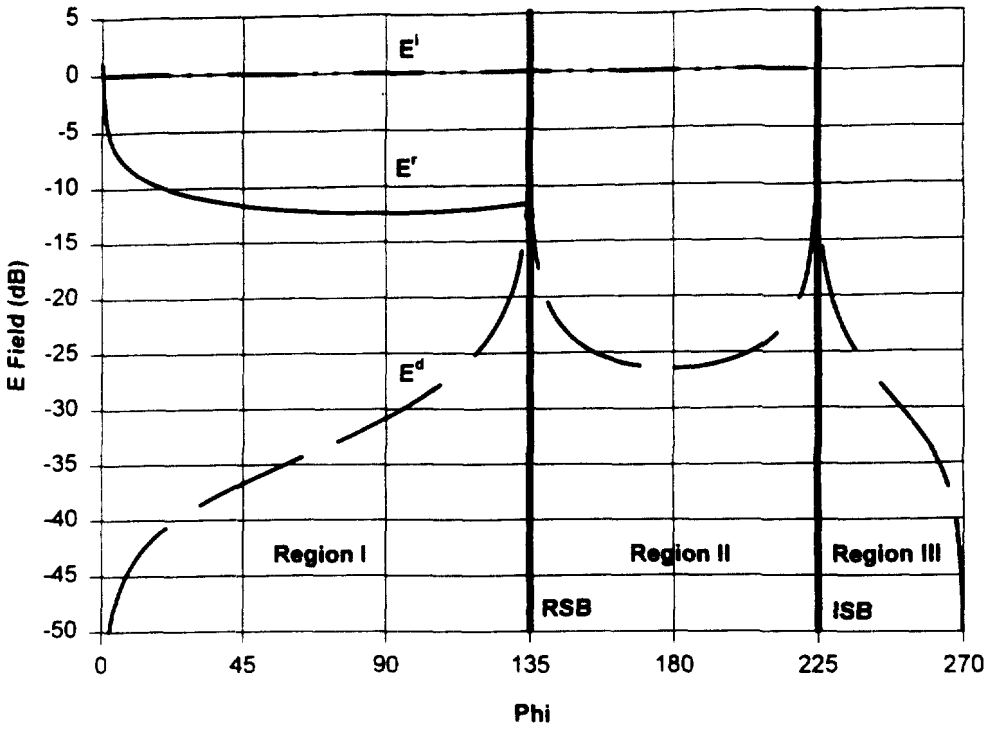

Exhibit A-7. 28.5 GHz incident, reflected and diffracted electric fields about building corner.

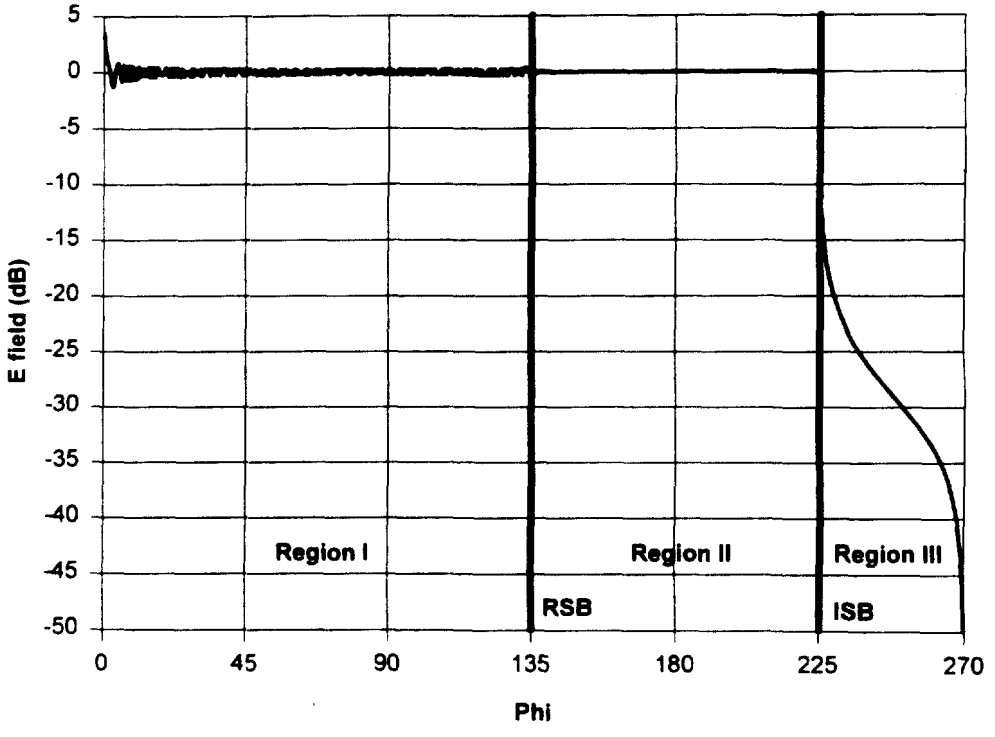

Exhibit A-8. 28.5 GHz total electric field about building corner.

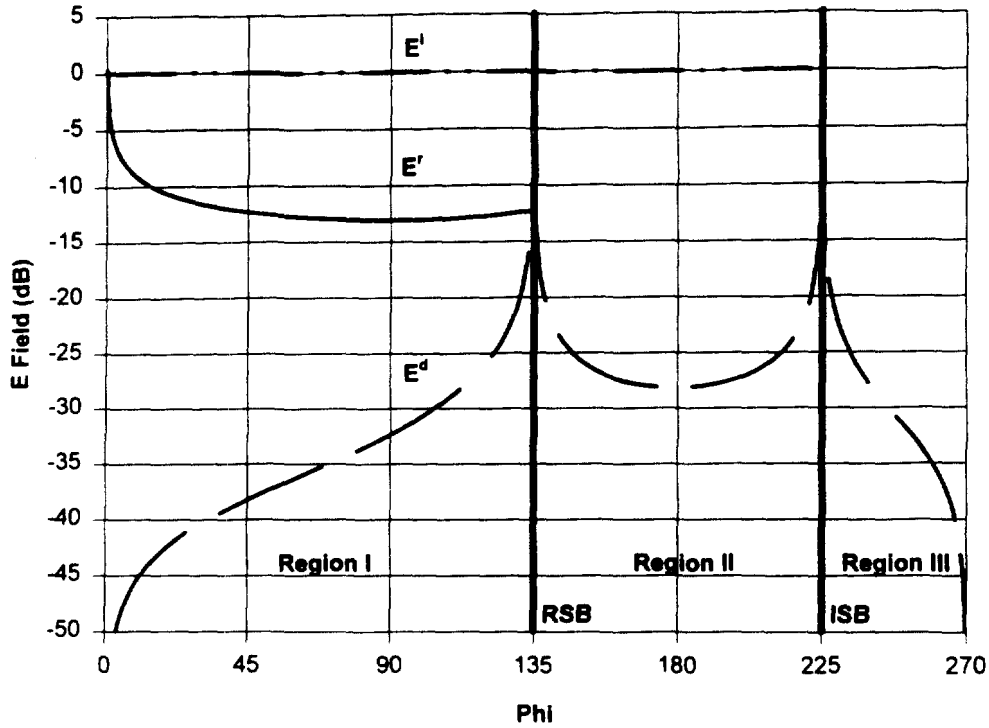

Exhibit A-9. 41.5 GHz incident, reflected and diffracted electric fields about building corner.

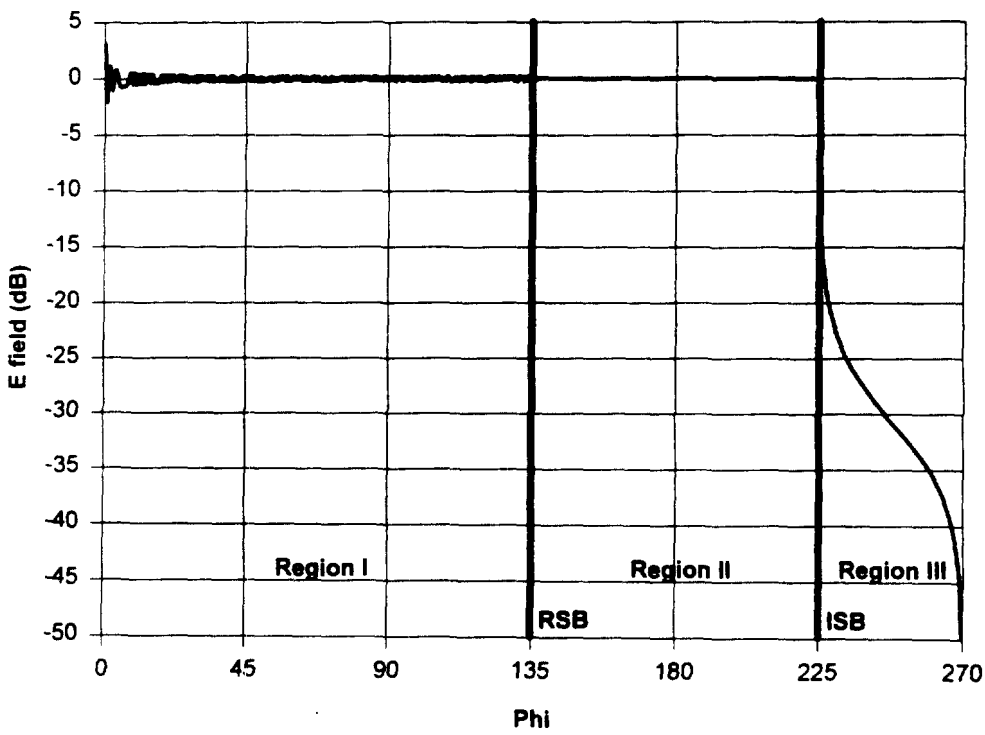

Exhibit A-10. 41.5 GHz total electric field about building corner.

Exhibit A-9 illustrates the 41.5 GHz incident, reflected, and diffracted electric field values for receiver locations about the building corner. The field patterns are very similar to the field patterns for 28.5 GHz. Both the reflected field and diffracted field patterns are basically the same shape as 28.5 GHz. Unless the receiver location is very close to the building, the reflected field is about 13 dB below the incident field. The diffracted field (neglecting the transition regions) peaks around ϕ equaling 180 degrees when the diffracted field is about 28 dB below the incident field. Exhibit A-10 illustrates the 41.5 GHz total electric field values at observation points about the building corner. And the total electric field pattern is very similar to the pattern for 28.5 GHz. Thus, the same conclusions are drawn for 41.5 GHz as were drawn for 28.5 GHz.

For 28.5 GHz the reflected field is approximately 11 dB below the incident field, and the diffracted field is at least 26 dB below the incident field. Meanwhile, for 41.5 GHz the reflected field is approximately 13 dB below the incident field, and the diffracted field is at least 28 dB below the incident field. The reflected and diffracted fields for both frequencies have almost identical radiation patterns except that 41.5 GHz reflected and diffracted fields are approximately 2 dB further below the incident fields than at 28.5 GHz. Thus, for both frequencies the diffracted field has a steep roll-off in the incident shadow region. This roll off is approximately 1 dB per degree. In conclusion, the total field electric field value is more sensitive to location than to frequency.